

Suppression of toxic transgene expression by optimized artificial miRNAs increases AAV vector yields in HEK-293 cells

Gina Blahetek,¹ Christine Mayer,¹ Johannes Zuber,^{2,3} Martin Lenter,¹ and Benjamin Strobel¹

¹Drug Discovery Sciences, Boehringer Ingelheim Pharma GmbH & Co. KG, 88397 Biberach an der Riss, Germany; ²Research Institute of Molecular Pathology (IMP), Vienna BioCenter (VBC), 1030 Vienna, Austria; ³Medical University of Vienna, Vienna BioCenter (VBC), 1030 Vienna, Austria

Adeno-associated virus (AAV) vectors have become the leading platform for gene delivery in both preclinical research and therapeutic applications, making the production of high-titer AAV preparations essential. To date, most AAV-based studies use constitutive promoters (e.g., CMV, CAG), which are also active in human embryonic kidney (HEK)-293 producer cells, thus leading to the expression of the transgene already during production. Depending on the transgene's function, this might negatively impact producer cell performance and result in decreased AAV vector yields. Here, we evaluated a panel of diverse microRNA (miRNA)-based shRNA designs to identify a highly potent artificial miRNA for the transient suppression of transgenes during AAV production. Our results demonstrate that insertion of miRNA target sites into the 3' UTR of the transgene and simultaneous expression of the corresponding miRNA from the 3' UTR of conventional AAV production plasmids (rep/cap, pHelper) enabled efficient silencing of toxic transgene expression, thereby increasing AAV vector yields up to 240-fold. This strategy not only allows to maintain the traditional triple-transfection protocol, but also represents a universally applicable approach to suppress toxic transgenes, thereby boosting vector yields with so far unprecedented efficiency.

INTRODUCTION

Due to their properties to elicit limited cytotoxicity,¹ allow for long-term transgene expression,^{2,3} and target a wide range of different tissue types,^{4–8} adeno-associated virus (AAV) vectors currently represent the most attractive platform for gene delivery in both therapeutic applications and preclinical research.

Traditionally, AAVs are either produced in baculovirus-infected Sf9 insect cells⁹ or in human embryonic kidney (HEK)-293 cells. Despite increasing successes in the development of stable packaging/producer cell lines (reviewed in Merten¹⁰), transiently transfected HEK-293 cells still represent the most commonly used platform for AAV production. Usually, production is based on transient transfection of three plasmids: (1) AAV replication (rep) and capsid (cap) plasmid (rep/cap), encoding genes for genome amplification and viral capsid formation, respectively; (2) helper plasmid (pHelper), encoding adenoviral proteins E2A, E4, and VA for efficient AAV packaging,

and (3) an expression cassette-harboring plasmid, minimally existing of a promoter, transgene and polyA signal, flanked by inverted terminal repeats (ITRs).¹¹ Since many AAV-based studies use constitutive promoters (e.g., cytomegalovirus [CMV], CAG promoters¹²) that are also active in HEK-293 cells, the transgene to be packaged is already expressed during the production process. In exploratory research, where transgene effects tend to be poorly characterized, their expression might exert cytotoxic or antiproliferative effects on the producer cells. Furthermore, in some cases, for example, for oncolytic virotherapy, cytotoxic transgenes are even desired. However, in both cases, transgene expression during the production process represents an unnecessary byproduct that may impact HEK-293 cell performance, thereby resulting in decreased or insufficient AAV vector yields.

Different approaches have been previously reported by us and others to suppress transgene expression during AAV vector production, including post-transcriptional silencing of transgene expression by a self-cleaving riboswitch integrated within the expression cassette,¹³ and the insertion of binding sites for naturally occurring microRNAs (miRNAs) within the cassette's 3' UTR.¹⁴ While both approaches led to increased AAV vector yields, they also entail disadvantages. For example, riboswitches might exert basal cleavage activity that slightly reduced AAV-mediated transgene expression also in the absence of ligand (approximately 33% lower expression in Strobel et al.¹³). Similarly, the insertion of binding sites for naturally occurring miRNAs into the transgene expression cassette, as described by Reid et al.,¹⁴ causes transgene suppression in tissues, where respective miRNAs are expressed.

We, therefore, reasoned that the use of non-mammalian or artificial miRNAs (amiRs) that are not endogenously expressed in mammalian organisms, together with engineered miRNA target sites in the 3' UTR of the toxic transgene, could provide a robust system to suppress

Received 19 February 2024; accepted 7 June 2024;
<https://doi.org/10.1016/j.omtm.2024.101280>.

Correspondence: Benjamin Strobel, Drug Discovery Sciences, Boehringer Ingelheim Pharma GmbH & Co. KG, 88397 Biberach an der Riss, Germany.
E-mail: benjamin.strobel@boehringer-ingelheim.com



transgene expression during AAV packaging, while leaving AAV functionality in downstream applications unaffected.

MiRNAs are a class of short (21–23 nt), non-coding RNAs that regulate gene expression post-transcriptionally by base pairing to complementary binding sites that are typically located within the 3' UTR of mRNAs.^{15,16} Depending on the complementarity, translation of mRNA is inhibited or decay of mRNA is induced.^{17,18} While classical RNA polymerase promoter III (e.g., U6)-driven short hairpin RNAs (shRNAs) can induce cytotoxic effects, due to oversaturation of the endogenous RNAi machinery,^{19–22} amiRs undergo natural Drosha/DGCR8 microprocessor processing, thereby strongly decreasing the risk of cellular toxicity.^{19,23} Moreover, since the packaging size of the AAV genome is restricted to approximately 4.7 kb, a further advantage of using miRNAs is the small size of the miRNA binding sites, enabling the introduction of multiple repeats into the 3' UTR of the AAV expression cassette without leaving a major footprint on the AAV genome size.

In our study, we evaluated miRNAs of different sources: (1) miRNA-based shRNAs with high *in silico* predicted efficiencies, based on SplashRNA scores,²⁴ expressed from an optimized miR-E backbone (“miR-F”)^{23,25}; (2) candidate sequences that were self-designed, according to generally applicable miRNA criteria; and (3) selected sequences from the non-mammalian organisms *Caenorhabditis elegans* and *Arabidopsis thaliana*. We then tested different approaches to express our lead miRNA sequence and investigated whether miRNA-mediated suppression of toxic transgenes during AAV production leads to increased AAV vector yields. To validate that the resulting miRNA target site-harboring AAV vectors maintain their functionality, we finally performed comparative *in vitro* transduction assays in different human and murine cell lines. In summary, we established highly efficient and transgene-independent designs that allowed for miRNA expression from conventional AAV production plasmids (rep/cap, pHelper) for the suppression of toxic transgenes during AAV production. As exemplified for the pro-apoptotic gene *BAX*, this strategy enabled efficient production of challenging AAV vector preparations with up to 240-fold higher yields.

RESULTS

SplashRNA-scored shRNA-miRs enable efficient transgene silencing *in vitro*

To identify an miRNA that enables effective transgene suppression during AAV production but shows no impact on AAV functionality in experimental applications, we aimed for miRNAs that are not endogenously expressed in mice and humans. To this end, we evaluated miRNAs of different sources: (1) artificial shRNA-miRs with high SplashRNA scores, (2) miRNAs from *Caenorhabditis elegans* and *Arabidopsis thaliana*, and (3) amiRs self-designed according to generally applicable miRNA design criteria.

The five miRNA-based shRNAs were selected based on their high *in silico* predicted efficiencies, according to the sequential classification algorithm SplashRNA.²⁴ These sequences were initially intended to

target murine *Kcnt2* (miR-F_01), *Cetn4* (miR-F_02), *Ankrd42* (miR-F_03), human *RORB* (miR-F_04), and murine *Khk* (miR-F_05). All SplashRNA-derived sequences were expressed using the miR-E backbone,²³ which was further modified by an A to G exchange (Figure 1A) supposed to disrupt an unfavorable basal bulge, according to miRNA design criteria published by Fang and Bartel.²⁵ This design is further referred to as miR-F. We additionally selected miRNA sequences from the non-mammalian organisms *C. elegans* (cel-miR39, cel-miR243) and *A. thaliana* (ath-miR159a, ath-miR416), which were expressed from their genomic primary miRNA (pri-miRNA) sequence. Finally, we self-designed amiRs (amiR-001/002/003) based on generally applicable criteria²⁶ and expressed them using the human miR-21 pri-miRNA backbone. The antisense guide sequences of all 12 miRNA candidates are shown in Table 1. Each pri-miRNA was cloned individually into a standard expression plasmid (pcDNA3.1), under the control of a CMV promoter (for details, see the Materials and methods). To analyze the silencing efficiency of each miRNA, we used a commercial dual luciferase reporter assay (Figure 1B) and inserted corresponding target sites for each miRNA into the 3' UTR of the Firefly luciferase (FLuc) reporter cassette. The second reporter on the plasmid construct, Renilla luciferase, was not modified, and therefore serves as a transfection and normalization control. HEK-293 cells were transiently co-transfected with a luciferase-miR target site plasmid and corresponding pcDNA-miR plasmid. At 48 h after transfection, Firefly and Renilla luminescence were measured.

Normalized luminescence revealed that the expression of all five SplashRNA-based, miR-F expressed miRNAs led to highly significant and efficient silencing of FLuc, with knockdown efficiencies of 94%–96%, as compared with the miRNA-free control (Figure 1C). amiR-001 and amiR-002 as well as cel-miR39 transfection also resulted in significant silencing of FLuc, however, at a lower potency, with remaining FLuc activities of 11%–60%. Expression of the remaining miRNAs did not result in efficient silencing of the luciferase reporter. Based on its high silencing efficiency, we chose miR-F_04 for further experiments, which hereafter is referred to as miR.

miRNA co-expression from AAV production plasmids enables efficient gene knockdown

After successful identification of a potent miRNA sequence, we next sought to apply it for transgene silencing in the AAV production context. In an attempt to avoid the transfection of an additional fourth (miRNA-expressing) plasmid during AAV vector production (on top of the conventionally used rep/cap, helper, and transgene plasmids), we inserted the 157mer miR scaffold sequence into the 3' UTR of the adenoviral helper gene VA (further referred to as pHelper-miR) or the 3' UTR of AAV6.2 or AAV2 *cap* genes (further referred to as pCap6.2.miR or pCap2.miR, respectively) (Figure 2A). To evaluate whether transgene silencing can be achieved by co-expressing miR from conventional AAV production plasmids, we tested these constructs using the dual luciferase reporter assay. To this end, HEK-293 cells were co-transfected with either pcDNA-miR, pHelper-miR, pCap6.2.miR, pCap2.miR, or a corresponding empty vector

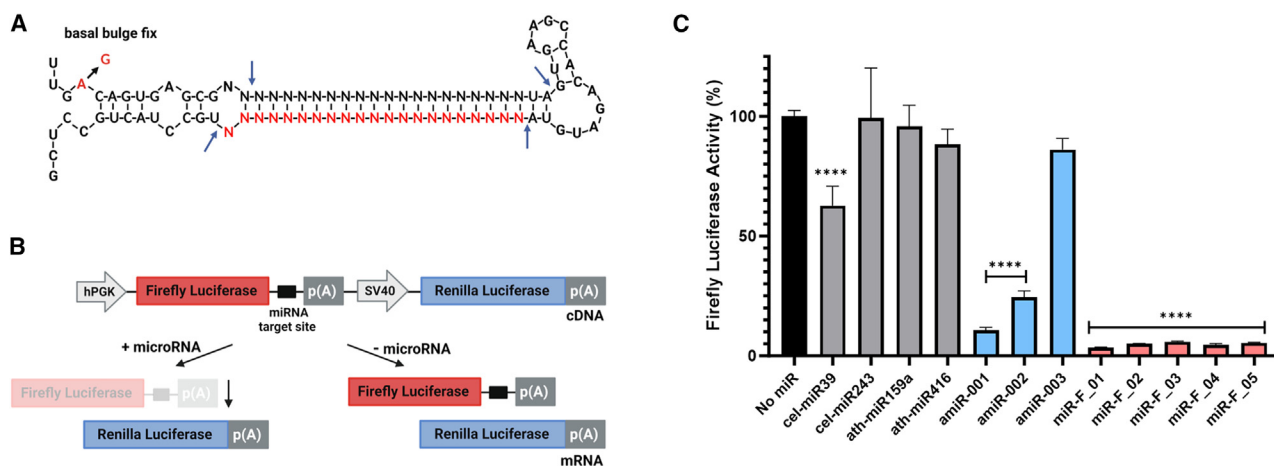


Figure 1. Evaluation of non-mammalian or artificial miR silencing efficiency

(A) Secondary structure of miR-E backbone. The optimized miR-F backbone is generated by substitution of nucleotide A by G, which results in a basal bulge fix, according to Fang and Bartel.²⁵ The position of the guiding strand is indicated in red letters. Cutting positions for miRNA processing nuclease Dicer are indicated by blue arrows. Created with BioRender.com. (B) Scheme of dual luciferase assay. In presence of a functional miRNA, expression of FLuc is decreased, whereas constitutive Renilla luciferase serves as a control for normalization. hPGK, human phosphoglycerate kinase promoter; p(A), polyadenylation signal; SV40, simian vacuolating virus 40 promoter. Created with BioRender.com. (C) miRNA efficiency assessment using the dual luciferase assay. One day after seeding, HEK-293 cells were transfected with the dual luciferase construct and either no miRNA (black), *C. elegans*, or *A. thaliana* (cel-miR39, cel-miR243 or ath-miR159a, ath-miR416; gray), artificial self-designed (amiR-001, amiR-002, amiR-003; blue) or high SplashRNA-ranked amiRs (miR-F_01, miR-F_02, miR-F_03, miR-F_04, miR-F_05; red). At 48 h after transfection, FLuc activity was measured and normalized to Renilla activity. $n = 3$ biological repetitions, mean \pm SD. **** $p < 0.0001$, by ordinary one-way ANOVA.

not expressing miR, and luciferase-miR target site reporter plasmids. At 48 h after transfection, Firefly and Renilla luminescences were measured. Normalized luminescence revealed that all tested constructs resulted in highly significant ($p < 0.0001$) and miRNA dose-dependent silencing of FLuc (Figure 2B), indicating effective miR expression from all tested constructs. To confirm these results with a second reporter and to further test functionality in the context of ITR-containing expression constructs, quadruplicate repeats of miR target sites were cloned into the 3' UTR of an ITR-flanked CMV-eGFP expression cassette (Figure 2C). Quantification of eGFP-positive cells 48 h after co-transfection of HEK-293 cells with either the miR-expression constructs or miR-free control and the eGFP-miR target site plasmid confirmed efficient transgene knockdown with all miR-expressing constructs (Figure 2D). However, in line with the luciferase data, pHelper.miR-mediated knockdown was less efficient (approximately 40% decrease in eGFP-positive cells) than that achieved by pCap.miR constructs (approximately 80% decrease in eGFP-positive cells (Figure 2E)). These results demonstrate effective silencing of luciferase and eGFP transgene expression by miR upon expression from conventional AAV production plasmids, with the greatest efficiencies achieved with rep/cap plasmid-based designs. Finally, we analyzed whether miR-mediated suppression of a toxic transgene can rescue the viability of AAV producing cells. To this end, we chose BCL2-associated X (BAX), which is a well-known pro-apoptotic gene,²⁷ and cloned quadruplicate repeats of miR target sites into the 3' UTR of an ITR-flanked CMV-BAX expression cassette. HEK-293 cells were then co-transfected with BAX-miR target site plasmid and increasing amounts of miR expressing plasmid. Quantification of vital HEK-293 nuclei revealed approxi-

mately 90% fewer vital nuclei upon BAX expression as compared with an untreated control. However, additional co-transfection of miR-expressing plasmid dose-dependently increased the number of vital nuclei up to approximately 75% (Figures 2F and 2G), indicating that cell viability can be rescued by miR-mediated toxic transgene suppression.

To further demonstrate that insertion of the miR target site within the transgene's 3' UTR does not impact the expression or functionality of the transgene in absence of miR, we transfected HEK293-cells with BAX, BAX-miRts and GFP-plasmids, respectively. Quantification of vital HEK-293 nuclei 48 h after transfection revealed approximately 30% fewer vital nuclei for both, cells transfected with 25 ng of BAX and BAX-miRts plasmid, respectively (Figures 3A and 3B). As expected, a further decrease in vital nuclei (up to approximately 90% at 100 ng DNA) was observed with increasing doses of DNA for both constructs, indicating that the insertion of miR target sites within the 3' UTR of the transgene has no impact on transgene functionality.

miR-mediated suppression of toxic transgene expression increases AAV vector yields

During the production of AAVs in HEK-293 cells, the transgene to be packed is expressed as an unintended side product that might impact HEK-293 cell viability in case of cytotoxic, anti-proliferative, or pro-apoptotic transgene effects, thereby decreasing AAV vector yields. To address our hypothesis that amiR-mediated suppression of transgene expression during AAV vector production leads to increased viral vector yields, we generated ITR-flanked expression cassettes

Table 1. Guiding strand sequences of screened miRNAs

Name of miRNA	Guiding miRNA sequence (5'-3')	miRNA target sequence
cel-miR39	UCACCGGGUGUAAAUCAGCUUG	CAAGCUGAUUUACACCCGGUGA
cel-miR243	CGGUACGAUCGCGCGGGAUAUC	GAUAUCCCGCCGCGAUCGUACCG
ath-miR159a	UUUGGAUUGAAGGGAGCUCUA	UAGAGCUCCCUUCAAUCCAAA
ath-miR416	GGUUCGUACGUACACUGUUCA	UGAACAGUGUACGUACGAACC
amiR-001	UGAGUUGAUAGCAGUAGUCCAA	UUGGACUACUGCUAUAACUCA
amiR-002	UCUCUUAUCACUGAACCAUCA	UUGAUGGUUCAGUGAUAGAGA
amiR-003	UGUCAUCUUCUUUCGGUUUCAG	CUGAAACCGAAAAGAAGAUACA
miR-F_01	UUAAGUUUCAAUAUGAUCUGUA	UACAGAUAUUUUGAAACUAAA
miR-F_02	UUUAAAAACAUUUCAUCUGGA	UCCAGAUGAAAUGUUUUUAAA
miR-F_03	UAAUCAUCAUGAUCUUCUGGA	UCCAGAUGAUCUGAUGAUUUA
miR-F_04	UAUAUUUGAACAAUACACAGGA	UCCUGUUGAUGUUCAAAUAUA
miR-F_05	UUUAUAUGAUUUUAUCCUCAC	GUGAGGAUAAAUAUAUAUA

harboring either a non-toxic eGFP, a slightly toxic MT-ND4 or a highly toxic BAX transgene under the control of a CMV promoter, and quadruple miR target sites within the transgenes' 3' UTR. The mitochondrial gene NADH dehydrogenase subunit 4 complex I (MT-ND4), which is currently in a phase 3 clinical trial (NCT03293524; [ClinicalTrials.gov](https://clinicaltrials.gov)) for an AAV2-based treatment of Leber's hereditary optic neuropathy, was previously reported to decrease AAV yields.¹⁴ The pro-apoptotic gene BAX has previously been shown to prevent efficient AAV production when expressed from constitutively active promoters.¹³ We then used these plasmids to produce AAVs of serotypes 2 or 6.2 in presence of miR, expressed from either an additional fourth plasmid (pcDNA.miR), the adenoviral pHelper (pHelper.miR), or the rep/cap plasmid (pCap.miR). The standard production setup without any additional miR expression served as a control. After iodixanol- and ultrafiltration-based purification, the titer of each AAV vector production (4-layer CELLdisc, 1,000 cm² culture area each) was determined by ITR-based digital PCR (dPCR).

Artificial miR-mediated silencing of non-toxic eGFP expression during AAV production revealed moderate, non-significant differences in AAV vector yield for pCap6.2.miR productions and for pcDNA.miR or pHelper.miR productions, respectively, compared with conventional control productions in the absence of miR (Figure 4A). Silencing of MT-ND4 expression during AAV vector production in HEK-293 cells led to a significant 1.8-fold increase of vector yields for pCap2.miR productions ($p = 0.0139$) and a 1.6-fold increase for pHelper.miR production ($p = 0.0408$) compared with control production. AAV yields for the four-plasmid approach using pcDNA.miR were not significantly increased (Figure 4B). Finally, we evaluated miR expression for the proapoptotic transgene BAX.

First, we examined the impact on vector yields when packaging the BAX expression cassette into serotype AAV6.2. Remarkably, the yields of AAV-BAX vectors increased by 117-fold for pCap6.2.miR productions, 73-fold for pHelper.miR productions, and 50-fold for

pcDNA.miR productions ($p < 0.0001$), compared with control productions in the absence of miR and miR-targeting sites (Figure 4C). To further confirm that the miR effect is serotype independent, we packaged the BAX-miR target site expression cassette into serotype AAV2. Here, the yields increased 74-fold for pCap2.miR productions ($p < 0.001$), 23-fold for pHelper.miR (not significant), and 46-fold for pcDNA.miR productions ($p = 0.0164$), compared with conventional productions (Figure 4D).

An alternative approach to suppress transgene expression on the post-transcriptional level during AAV vector production has been previously reported by our group.¹³ Here, a conditionally self-cleaving aptazyme riboswitch called GuaM8HDV was integrated into the 3' UTR of the transgene expression cassette.¹¹ In the absence of its ligand guanine, the riboswitch remains intact, maintaining mRNA integrity and gene expression. However, upon the addition of guanine to the culture medium, self-cleavage of the riboswitch is initiated, leading to a loss of the poly(A) tail and corresponding mRNA degradation, thereby switching off transgene expression (Figure 4E). To compare our new, amiR-mediated approach to the previous riboswitch-based strategy, we conducted a side-by-side experiment, where both approaches were tested in comparison with a conventional (riboswitch and miRNA-free) production. As the greatest increases of AAV vector yields were achieved by expressing miR from the 3' UTR of the AAV6.2 rep/cap plasmid (Figure 4C), we used this setup for comparison.

Using the conventional proapoptotic CMV-BAX expression construct in the absence of miR or guanine, only very low AAV yields were obtained (average total yield from 4-layer CELLdiscs (1,000 cm² culture area): 9.6×10^9 vg, $n = 3$). In contrast, by guanine riboswitch-mediated silencing of BAX during AAV vector production, AAV vector yields were increased 15-fold to 1.4×10^{11} vg. Strikingly, by using the new artificial miR-mediated strategy, an additional 16-fold increase over the riboswitch approach was achieved, resulting in in average AAV vector yields of 2.3×10^{12} vg per 1,000 cm² culture

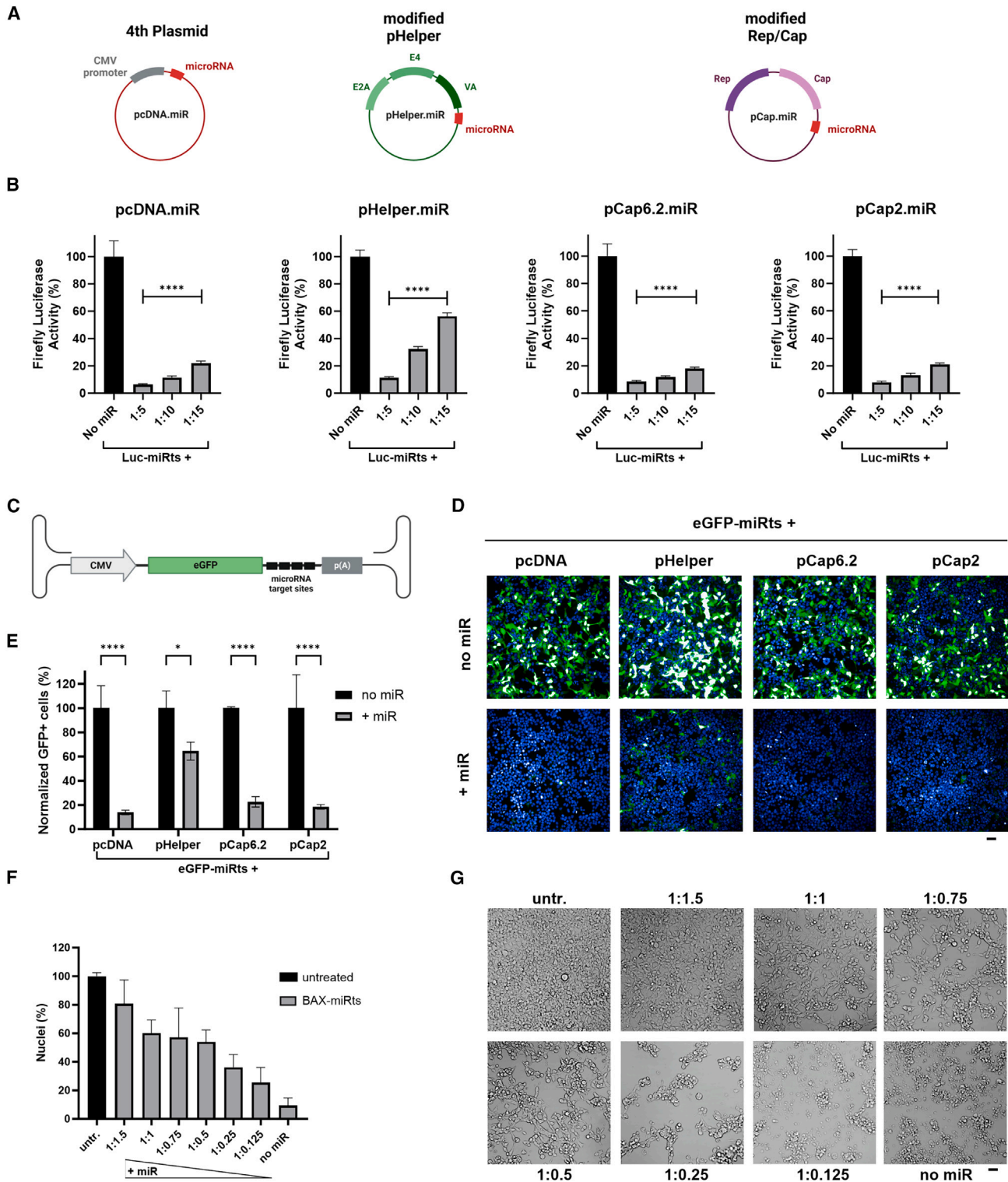


Figure 2. Evaluation of miRNA silencing efficiency, co-expressed from conventional AAV production plasmids

(A) Representation of artificial miR-F-04 expressing plasmids. (Left) pcDNA3.1 vector expressing 157mer miR-F-04 (further referred to as miR) under the control of a CMV promoter (further referred to as pcDNA.miR). (Middle) modified pHelper, co-expressing miR from the downstream sequence (3' UTR) of the adenoviral helper gene VA (further

(legend continued on next page)

area and an overall 240-fold increase (Figure 4F, red bar). Taken together, these results show that transient silencing of toxic transgenes by artificial miR-mediated RNAi is a highly efficient and universally applicable approach to increase AAV vector yields.

miR target site-harboring AAV vectors maintain bioactivity *in vitro*

Improved AAV vector yields are only beneficial, if miR target site-harboring AAV vectors maintain their ability to efficiently express transgene. Therefore, to assess the impact of repeated miR target site insertions on transgene expression, we transduced human and murine cell lines, originating from different tissues, with increasing amounts of AAV6.2-eGFP, with or without miR target sites in the 3' UTR. Depending on the cell line and corresponding AAV expression kinetics, eGFP expression was determined 48 h or 72 h after transduction, by quantification of eGFP-positive cells. As expected, overall, no significant differences were observed between miR target site-harboring and conventional AAVs' transduction efficiency (Figure 5). The only statistically significant ($p < 0.05$) differences in 3 of 15 comparisons were observed with the two lower doses in case of the murine Müller glia cell line Moorfields/Institute of Ophthalmology-Müller 1 (Mio-M1) (Figure 5C) ($p = 0.0338$ and $p = 0.0446$), and the high dose in the murine hepatocyte cell line FL83B (Figure 5E) ($p = 0.0465$), where miR-targeting site-harboring vectors showed slightly decreased transduction efficiencies. No differences were identified in HEK-293 cells, the human hepatocyte cell line HepG2, or the murine intestinal neuroendocrine cell line STC-1. Taken together, our data show that miR target site-harboring AAVs maintain their ability to efficiently express transgene *in vitro*.

DISCUSSION

Our study demonstrates that amiR-mediated silencing of transgene expression during AAV production in HEK-293 cells enables significant increases in AAV vector yields when packaging a highly cytotoxic transgene such as the proapoptotic protein BAX. The ability to efficiently package such genes is desirable for different reasons, for instance, applications in oncolytic virotherapy/suicide gene therapy, de-risking of vector production for sparsely characterized genes, or exploratory research, where the AAV-mediated expression of toxic genes could be used to deplete cells in a targeted fashion, similar to established diphtheria toxin receptor models.²⁸

Using the miR-free control construct, AAV-BAX yields were very low (1×10^{10} – 5×10^{10} vg), due to constitutive CMV-mediated BAX expression. In contrast, AAV yields were increased up to 240-fold when integrating miR target sites within the BAX expression cassette and co-expressing miR during AAV production (AAV6.2 and AAV2). Despite this drastic increase, however, AAV production efficiency of a non-toxic transgene production could not be reached (with AAV6.2-BAX reaching approximately 12% of AAV6.2-eGFP control vector yields, when comparing Figures 4A and 4C), indicating that the highly potent proapoptotic effect of BAX could not be fully blocked by the amiR.

The remarkable efficacy of the selected miRNA candidate in this work is likely due to two main reasons. First, we applied SplashRNA-scoring, a sequential classifier that was demonstrated to identify highly efficient shRNA sequences. Second, the miRNAs were expressed using an optimized miRNA scaffold, under the control of a strong, Pol II-driven CMV promoter.^{29,30} The previously reported miR-E backbone was originally intended to increase the precise generation of mature shRNAs for single copy-RNAi applications, such as shRNA-based library screens.²³ Pelosof et al.²⁴ demonstrated that high-scoring SplashRNA-predicted shRNAs, embedded into the miR-E backbone, mediate greater than 85% protein knockdown, when expressed from a single genomic integration. Given that our study used a plasmid transfection-based, and hence multi-copy setup, it is not surprising that the SplashRNA-predicted sequences mediated highly efficient protein knockdown, with efficiencies of 94%–96% (Figure 1). In turn, these high efficiencies might suggest that a decrease in the number of repetitive miR binding sites (four in the current design) could be approached in the future, to further fine-tune the system. Our amiR candidate miR-F_04 was initially predicted to target human RAR-related orphan receptor B (RORB), a DNA binding protein that has been shown to interact with proteins involved in neuronal differentiation as well as regulation of circadian rhythm (reviewed in Liu et al.³¹). To avoid any harmful effects on HEK-293 cells by the suppression of RORB, we validated the potential target gene as not being expressed in HEK-293 cells, according to the open access cell line section of the Human Protein Atlas.³² In addition, we did not observe any anomalies during AAV production in the cells' growth behavior or phenotype upon miR-F_04 expression.

referred to as pHelper.miR). (Right) Modified rep/cap plasmid, expressing miR from the downstream sequence (3' UTR) of the Cap gene (further referred to as pCap.miR). Created with BioRender.com. (B) Dual luciferase assay in HEK-293 cells. Cells were co-transfected with either different concentrations of empty (black) or miR-expressing (gray) plasmids and miR target sites (miRts) harboring dual luciferase plasmid (1:5, 1:10 and 1:15 indicate the molar ratio of miR-expressing to miRts plasmids). FLuc activity was normalized to Renilla luciferase activity. Statistical significance was determined for each miR concentration vs. the empty control. $n = 3$ biological repetitions, mean \pm SD. **** $p < 0.0001$, one-way ANOVA. (C) Scheme of AAV expression construct, containing quadruplicate repeats of miR target sites within the 3' UTR of a CMV-eGFP expression cassette, p(A), polyadenylation signal. Created with BioRender.com. (D) Representative fluorescent microscopy images of HEK-293 cells, 48 h after co-transfection with the AAV eGFP plasmid shown in (c) and either miR-expressing plasmids (+miR) or corresponding empty vector (no miR) at a molar ratio of 1. eGFP signal for all images was recorded for 100 ms. Blue staining: Hoechst33342 for vital nuclei identification. Scale bar, 50 μ m. (E) Quantification of eGFP-positive cells from (d). $n = 3$ biological repetitions, mean \pm SD. Two-way ANOVA. * $p < 0.05$ and **** $p < 0.0001$. (F) HEK-293 cells were either left untreated (untr.) or co-transfected with BAX-miRts plasmid and increasing concentrations of pCap6.2.miR (+miR) at molar ratios for BAX-miRts to miR-expressing plasmids of 1:0.125–1:1.5, as indicated). At 48 h after transfection, cells were stained with Hoechst33342 for vital nuclei identification and quantified by automated image analysis. $n = 3$ biological repetitions, mean \pm SD. (G) Representative microscopy images of (F). Numbers indicate the molar ratio of pCap6.2.miR plasmid to BAX-miRts plasmid, as in (F). Scale bar, 50 μ m.

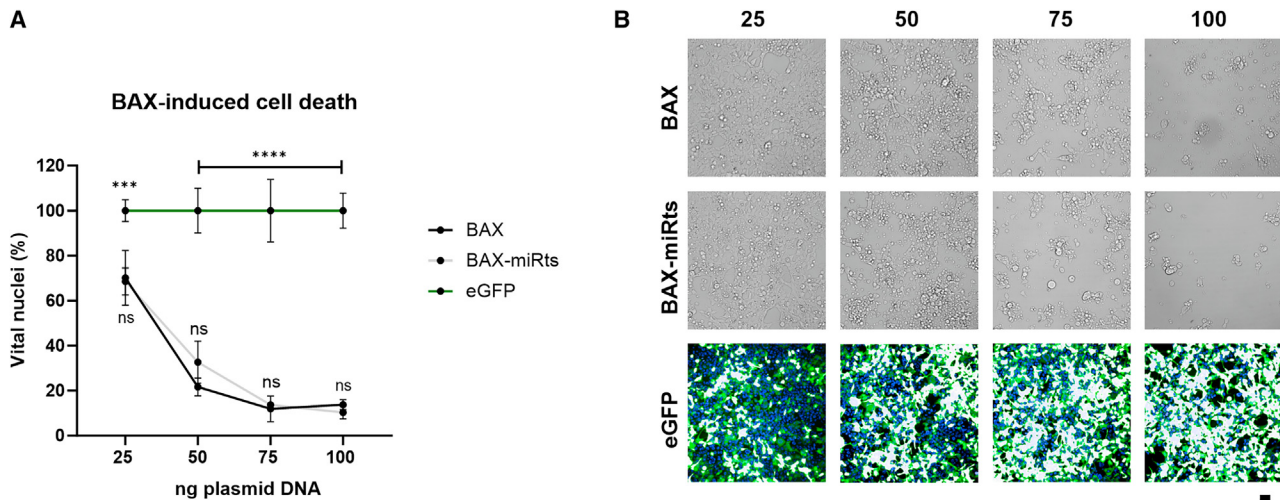


Figure 3. miRts-harboring BAX expression constructs maintain potency *in vitro*

(A) HEK-293 cells were transfected with increasing amounts (25, 50, 75, or 100 ng) of either BAX, BAX-miRts, or eGFP plasmids. At 48 h after transfection, cells were stained with Hoechst33342 and vital nuclei were quantified by automated image analysis. The percentage of vital nuclei is presented relative to vital nuclei under eGFP control conditions. $n = 3$ biological repetitions, mean \pm SD. Two-way ANOVA. *** $p < 0.001$ and **** $p < 0.0001$. (B) Representative microscopy images of (A). Numbers indicate the amount of each transfected plasmid in ng. Scale bar, 50 μ m.

Additional approaches have been previously reported by our group and others to suppress transgene expression on the post-transcriptional level during AAV vector production, by inserting small sequence sections within the 3' UTR of the transgene expression cassette: We previously used a self-cleaving aptazyme riboswitch placed into the 3' UTR of the transgene expression cassette. By addition of the riboswitch ligand guanine to the production process, self-cleavage of the riboswitch is initiated, which leads to a loss of the poly(A) tail and the degradation of the transgene mRNA during AAV production (Figure 4E). In the absence of the ligand, the riboswitch remains intact, maintaining mRNA integrity and gene expression, thereby enabling the use of riboswitch-containing AAVs under normal *in vitro* or *in vivo* conditions, where no exogenously added guanine is present.^{13,33} Comparable with our novel approach, Reid et al.¹⁴ used an miRNA-mediated strategy to silence transgene expression during AAV production. However, they inserted binding sites of naturally occurring miRNAs within the 3' UTR of the transgene, which are known to have high, tissue-specific expression levels: hsa-miR-373 (placenta), mmu-miR-122a (liver), and mmu-miR-367 (heart).¹⁴ Interestingly, both previously shown strategies mediated comparable, 23-fold and 22-fold increased AAV vector yields for BAX, respectively. Yet, they have not been as efficient as our novel artificial-miRNA based approach, that led up to a 240-fold AAV yield increase. Moreover, while a disadvantage of the guanine riboswitch lies in its basal cleavage activity that decreased AAV-mediated gene expression by 33% *in vivo* in the absence of ligand,¹³ a major drawback of using naturally occurring mammalian miRNAs is that AAV-mediated expression will be silenced in tissues expressing these miRNAs, thereby limiting the general applicability of this system. In contrast, by using amiRs and unique target sites, it is highly unlikely that AAV-derived mRNAs will be targeted by endogenously present

miRNAs. In fact, this assumption was confirmed in our experiments, using different murine and human cell lines, where AAV vectors harboring miR target sites expressed GFP with similar efficiency as the control constructs. Thus, by using amiRs to increase the yields of AAV vectors carrying cytotoxic transgenes, unintended transgene suppression by naturally occurring miRNAs is avoided, while AAV bioactivity is maintained.

While the use of cell- and tissue-specific promoters that show no or little expression in the production cell line HEK-293, such as the heart/cardiomyocytes specific cTnT promoter,³⁴ the CNS/neuron-specific synapsin-1 promoter,³⁵ or the liver/hepatocyte-specific LP1 promoter,³⁶ represents an alternative approach to lower transgene expression during vector production, most AAV-based studies use strong constitutive promoters. Examples include a CAG or CMV promoter, which enable a broad expression in different cell types and/or different target tissues of interest.¹² Therefore, using amiRs and their complementary target sites represents an effective approach, whenever broad expression of the transgene is desired, and the use of a tissue-specific promoter is not possible.

In the context of AAV production, transfection of a fourth plasmid (on top of the transgene, rep/cap, and pHelpers) to overexpress the miRNA would be the easiest approach. In practical terms, however, this requires additional plasmid DNA preparation and a modification of the transfection protocol (DNA amount, plasmid ratios). To circumvent this, we attempted to co-express our candidate miR from plasmids that are anyway required for AAV production: rep/cap and pHelper. By expressing the miR from the 3' UTR immediately downstream of the stop codon of the adenoviral VA gene in the pHelper, and the AAV *cap* gene in the rep/cap plasmid, respectively,

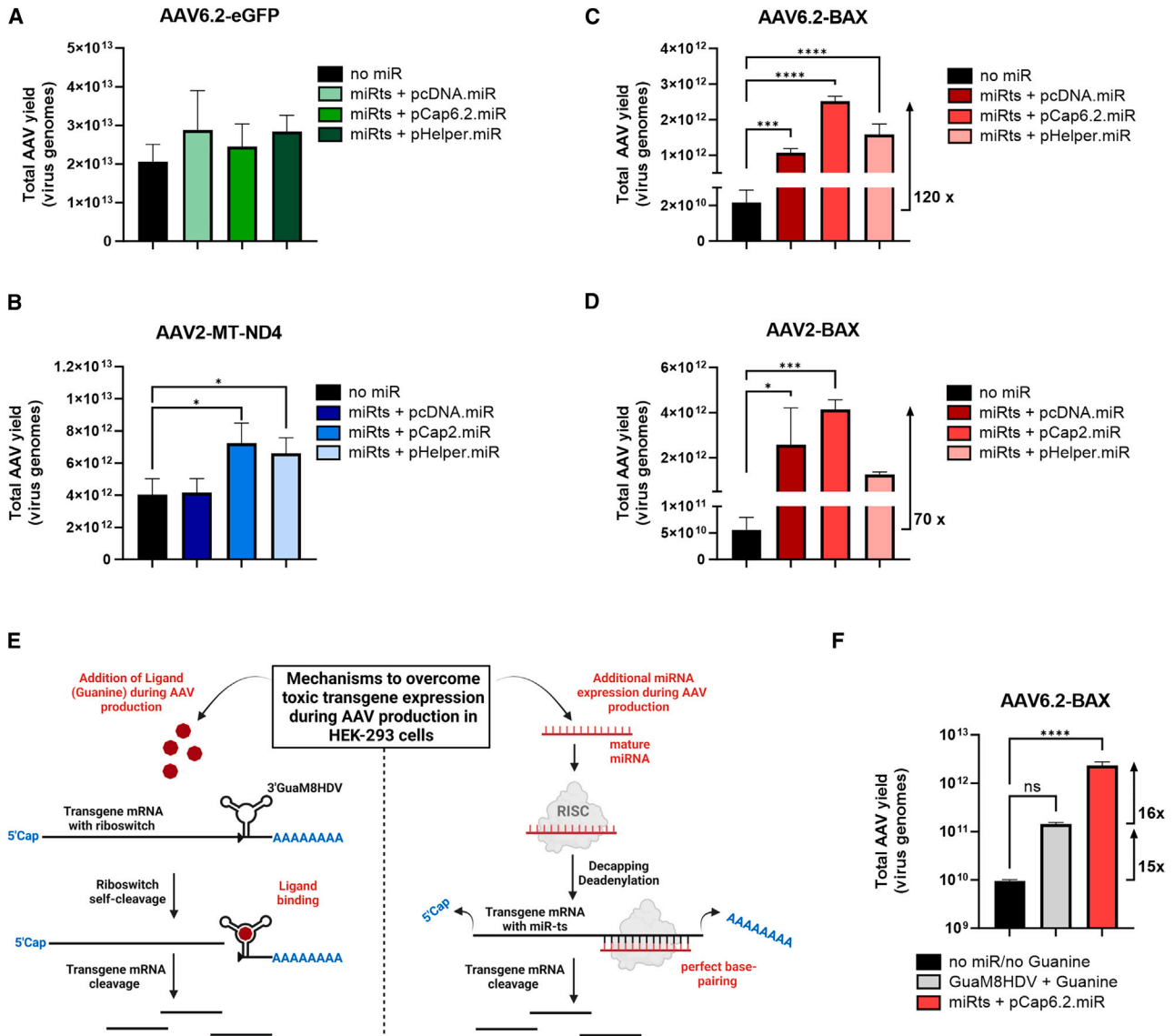


Figure 4. miRNA-mediated transgene silencing increases AAV vector yields

(A–D) To assess the impact of miR-based transgene silencing on AAV yields, either (A) CMV-eGFP, (B) CMV-MT-ND4 or (C and D) CMV-BAX AAV vectors were produced in HEK-293 cells by co-transfection of the corresponding miR target site-harboring transgene, rep/cap and pHelpers, under either standard conditions (no miR) or using miR-expressing pcDNA, pCap or pHelper variants, as indicated. Following vector purification by PEG-precipitation, iodixanol gradients and ultrafiltration, AAV vector genomes were quantified by ITR-based dPCR. Fold increases in vector yields are indicated for AAV2 and AAV6.2-CMV-BAX vectors. $n = 3$ CELLdiscs (1,000 cm² growth area) for each production condition, mean \pm SD. One-way ANOVA, * $p < 0.05$, *** $p < 0.001$ and **** $p < 0.0001$. (E) Scheme of two post-transcriptional mechanisms to overcome cytotoxic transgene expression during AAV production in HEK-293 cells. (Left) Scheme of AAV-GuaM8HDV construct design for riboswitch-mediated transgene suppression.¹³ The riboswitch was inserted into the 3' UTR of the transgene. Addition of the riboswitch ligand (guanine) to the AAV production process induces self-cleavage of the riboswitch, and subsequent cleavage and degradation of transgene mRNA. (Right) miRNA expression during the AAV production process leads to RNA-induced silencing complex (RISC) formation, and binding of the miRNA to target sites within the transgene's 3' UTR. miRNA-binding to the transgene mRNA leads to 5'-decapping and 3'-deadenylation of transgene mRNA, subsequently triggering mRNA cleavage. Created with [BioRender.com](#). (F) AAV6.2-CMV-BAX vectors were produced under either conventional (no miR/no guanine) conditions or using a self-cleaving riboswitch-containing construct induced by 150 μ M guanine, or the CMV-BAX-miRts construct and pCap-mediated miR-expression. After vector purification, AAV vector genomes were quantified by ITR-based dPCR. $n = 3$ CELLdiscs (1,000 cm² growth area) for each production condition; mean \pm SD. One-way ANOVA, **** $p < 0.0001$. ns, not significant.

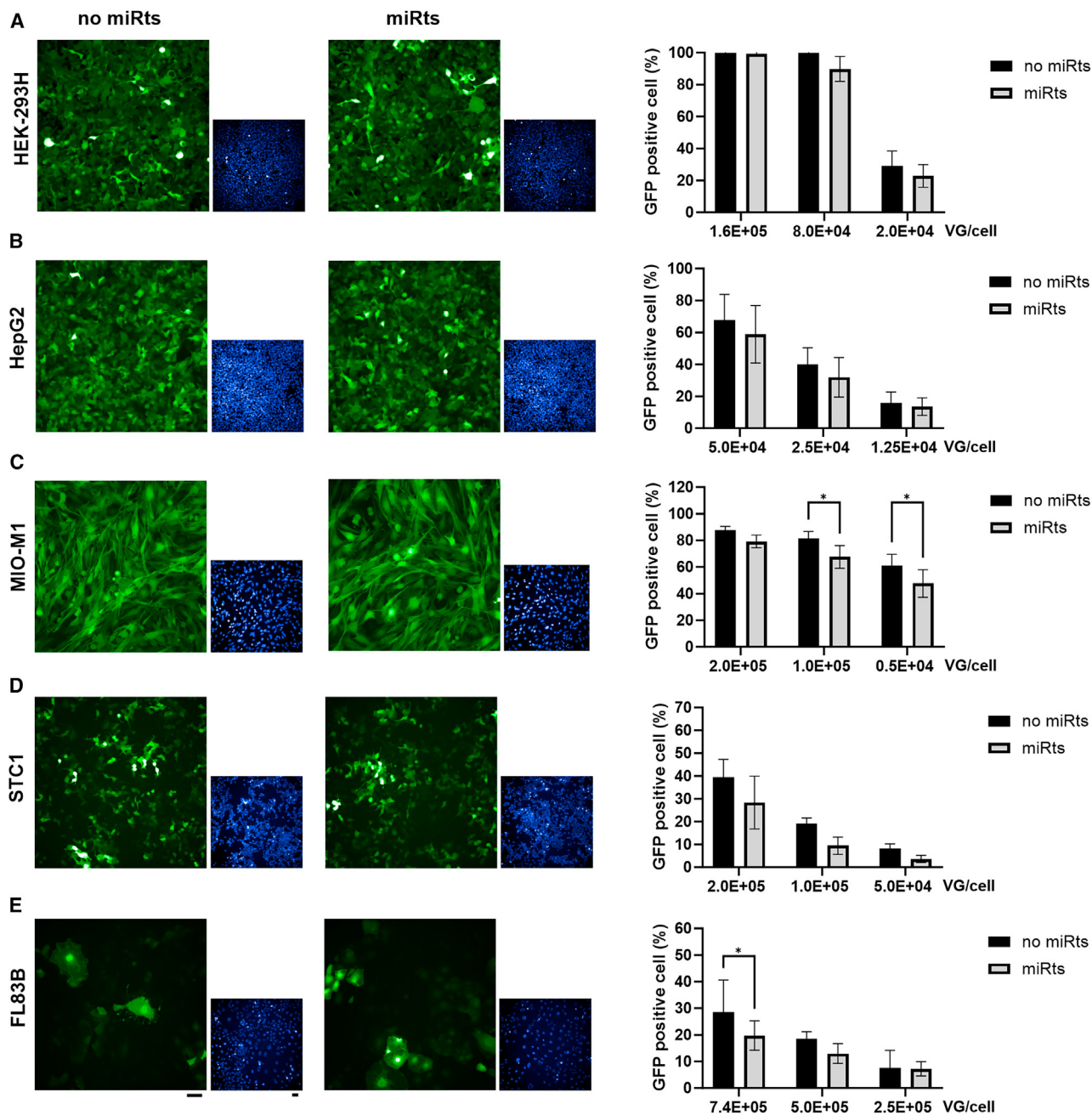


Figure 5. miRts-harboring AAV vectors maintain bioactivity *in vitro*

Human (A–C) and murine (D–E) cell lines were transduced with indicated amounts of viral genomes per cell of AAV6.2-eGFP (no miR target site) or AAV6.2-eGFP-miRts (viral genome contains miR target site). At 48 h or 72 h after transduction, eGFP-positive cells were quantified by automated image analysis. Representative fluorescent microscopy images and corresponding Hoechst33342 images are shown. eGFP fluorescence was recorded for 100 ms. Scale bar, 50 μ m. $n = 3$ biological repetitions for each concentration, mean \pm SD. Two-way ANOVA, * $p < 0.05$.

the miR undergoes processing as a natural substrate of the miRNA processing pathway. The effective silencing of the luciferase and GFP reporters clearly demonstrated successful co-expression and processing into a functional miRNA (Figure 2).

Similar to the four-plasmid approach, pHelper-based miR expression mediated by approximately 50-fold higher yields during AAV production (BAX). pHelper-based expression represents an attractive approach, especially because it is universally applicable, independent

of the AAV capsid choice. Still, the strongest improvement of AAV vector yields was observed by co-expressing the miRNA from the 3' UTR of the *cap* gene. This not only allows to stay with the traditional three-plasmid production protocol, but also additionally improved AAV vector yields approximately 2.4-fold, compared with the pHelper approach. An additional way to express miR during the AAV production process is the generation of a stably miR-expressing HEK-293 production cell line, which is currently under evaluation in our lab.

Finally, in addition to their application during AAV production, miRNAs also represent an attractive tool to silence or even induce gene expression in *in vivo* applications. The usage of our miRNA-target site harboring AAV expression cassette allows for silencing of transgene expression, for example, by administration of miRNA mimics, synthetic small RNA duplexes, that behave similarly to endogenous miRNAs and thus mediate gene silencing.³⁷ Temporary silencing may be necessary, for example, when consistent transgene expression would have cytotoxic effects on targeted organs, or to study temporal gene expression effects, when using AAVs as a research tool.³⁸ A strategy to conditionally induce AAV-mediated transgene expression by shRNAs was recently demonstrated by Subramanian et al., who generated a self-silencing AAV transgene expression cassette. Here, the expression of the transgene is induced by inhibiting the silencing shRNA via a high-affinity oligonucleotide complementary to the shRNA sequence.³⁹

In summary, our data demonstrate that the expression of an optimized amiR from the 3' UTR of conventional AAV production plasmids is a highly efficient and universally applicable approach to suppress toxic transgenes during AAV production, thereby enabling efficient production of AAV vectors harboring challenging transgenes. In addition to its use for AAV production optimization, the highly efficient miRNA approach might further be extended to temporal regulation of therapeutic transgene expression *in vivo*.

MATERIALS AND METHODS

Artificial miRNAs

Sequences for potent miRNA-based shRNAs were selected based on a high SplashRNA score.²⁴ Potential target genes of top candidates of SplashRNA score ranking were validated to be not expressed in HEK-293 cells in an open access cell line section of the Human Protein Atlas³² to avoid suppression of potential target transcripts and associated effects on the AAV production cell line (see Table 1 for sequence information).

The previously described miR-E backbone²³ was slightly modified by substitution of nucleotide A by G at position 2 to fix an unfavorable basal bulge (based on design criteria published by Fang and Bartel²⁵) to further enhance pri-miRNA processing, and subsequently called miR-F. Sequences of selected miRNA-based shRNAs were expressed from optimized 157mer miR-F scaffolds (sequence as in Figure 1A, flanked by 5' TCGACTTCTTAACCCAACAGAAGGCTCGAGAA GGTATATTGCTG and 3' GACTTCAAGGGGCTAGAAATTCGA).

Cell culture

The human Müller cell line Mio-M1⁴⁰ was obtained from the UCL Institute of Ophthalmology. Human HEK-293H cells (acCELLerate), human MioM1 and murine STC-1 (ATCC, #CRL-3254) cells were cultured in DMEM high-glucose with GlutaMAX (Life Technologies) supplemented with 10% fetal bovine serum (FBS) (Life Technologies). Human HepG2 cells (ATCC; #HB-8056) were cultured in MEM medium (Life Technologies) supplemented with 10% FBS and 1% NEAA. Murine FL83B cells (ATCC; #CRL-2390) were cultured in F-12K Nutrient Mix (Life Technologies) supplemented with 10% FBS. All cell lines were cultured at 37°C and 5% CO₂.

Plasmid constructs

Selected miRNA sequences from either *C. elegans* or *A. thaliana* (see Table 1), embedded in 200–250 bp of upstream and downstream genomic flanking regions, predicted amiR sequences, embedded in optimized 157mer miR-F scaffold and self-designed miRNA sequences, embedded in 250 bp of upstream and downstream genomic flanking regions of hsa-miR-21 were synthesized (Thermo Fisher Scientific). Sequences were cloned into BamHI and XhoI restriction sites of standard mammalian expression vector pcDNA3.1. Selected miR-F_04 sequence was subcloned between the *cap* gene stop codon and first polyA signal of AAV rep/cap plasmids AAV2/2 and AAV2/6.2 using BclI and BshTI restriction sites (constructs referred to as pCap2.miR or pCap6.2.miR) or into SalI and NdeI restriction sites of pHelper (AAV Helper-free system, Agilent; plasmid construct referred to as pHelper.miR). Oligonucleotide pairs, that contain miRNA target sites were ordered (Sigma Aldrich), annealed and cloned into PstI and XbaI restriction sites of pmiRGLO vector (Promega). Quadruplicate miRNA target site of miR-F74014 was synthesized (Thermo Fisher Scientific) and cloned into the 3' UTR of transgene cassette of pFB-eGFP, pAAV-BAX or pAAV-MTND4, using HindIII and XhoI restriction sites.

Dual luciferase assays

The day before transfection, HEK-293H cells were seeded in a white multiwell plate to reach approximately 70% confluence on the day of transfection. For initial testing of miR silencing efficiency, cells were transfected with 50 ng pmiRGLO-miRts plasmid constructs and equimolar amounts of corresponding pcDNA-miRNA expression plasmids, using Lipofectamine 2000 transfection reagent (Thermo Fisher Scientific). For evaluating the silencing efficiency of miR-F_04, co-expressed from AAV production plasmids, cells were transfected with 50 ng pmiRGLO-miRts plasmid construct and equimolar amounts of miR-expressing plasmids (pcDNA.miR, pHelper.miR, pCap6.2.miR, or pCap2.miR; each miR expressing plasmid was diluted 1:5, 1:10, or 1:15 with corresponding empty vector). At 48 h after transfection, samples were processed according to manufacturer's instructions (Dual-Glo Luciferase Assay System, Promega) and luminescence was measured. Firefly luminescence was normalized to Renilla luminescence.

Transfection for GFP and BAX assays

The day before transfection, HEK-293H cells were seeded in a black ViewPlate (PerkinElmer) to reach about 70% confluence on day of

transfection. We co-transfected 50 ng pAAV-GFP-miRts plasmid with equimolar amounts of pcDNA.miR, pHelper.miR, pCap6.2.miR or pCap2.miR, respectively, or corresponding empty vector (no miR). At 48 h after transfection, GFP intensity was measured by microscopy. To assess the effect of miR in the context of BAX overexpression, HEK-293H cells were co-transfected with 100 ng of pAAV-BAX-miRts plasmid miR-expressing plasmid at molar ratios for BAX-miRts plasmid to pCap6.2.miR plasmid of 1:1.5, 1:1, 1:0.75, 1:0.5, 1:0.25, 1:0.125, or transfected with pAAV-BAX-miRts plasmid only. To assess the effect of toxic transgene expression in presence of miR target site and absence of miR, HEK-293H cells were transfected with increasing amounts of pAAV-BAX-miRts or pAAV-BAX plasmid, as indicated. At 48 h after transfection, cells were stained with Hoechst33342 to quantify vital nuclei by automated image analysis (see below).

AAV transduction

The day before transduction, cell lines were seeded in a black ViewPlate (PerkinElmer) to reach about 70% confluence on the day of transduction. AAV preparations were diluted with DPBS to 1×10^8 vg/ μ L. Diluted AAV preparations were added to the plates to achieve the specified vg/cell. Cells were incubated for 2 or 3 days at 37°C, 5% CO₂, before measuring eGFP intensity by fluorescence microscopy and automated image analysis.

Fluorescence microscopy and automated image analysis

To detect GFP-positive cells, ViewPlates were processed with an Opera Phenix High-Content Screening System (PerkinElmer). Five evenly distributed 646 μ m² fields were measured per 96-well plate with Brightfield, GFP (excitation at 488 nm, emission at 500–550 nm), and Hoechst33342 (excitation at 405 nm, emission at 435–480 nm) channels. Exposure settings for the GFP channel were fixed to 100 m, and 300 m for Brightfield and Hoechst33342. Resulting pictures were analyzed with the Columbus Image Data Storage and Analysis System (PerkinElmer). First, the Hoechst33342 signal was used to automatically detect vital nuclei. Uneven or overlapping nuclei were excluded. To measure GFP intensities of the vital nuclei area, GFP background signal levels were determined by quantifying the GFP signal of an untransduced well. Then, GFP intensities of vital nuclei areas of transduced wells were measured and averaged to obtain the final GFP intensity score. Percentages of GFP-positive and vital nuclei areas were determined for each sample.

AAV production

All AAVs were produced as described previously.⁴¹ Briefly, frozen aliquots of high-density HEK-293H cells (AcCELLerate) were thawed and 1.5×10^7 cells/4-layer CELLdisc (Greiner Bio-One) were seeded 3 days before transfection in DMEM, containing 10% FBS. on the day of transfection, medium was changed to DMEM, containing 5% FBS and Adenoviral helper (AAV helper-free system; Agilent), respective rep/cap plasmids and a plasmid containing an AAV2-ITR flanked, self-complementary CMV-based expression cassette (transgenes as indicated in figure legends) were co-transfected by calcium phosphate transfection. At 5–6 h after transfection, media was changed and re-

placed with fresh DMEM containing 5% FBS. After 3 days, cells were detached by the addition of EDTA and collected by centrifugation. High-salt lysis buffer and three freeze/thaw cycles were used to release the AAV particles from the cells. Genomic DNA and remaining plasmid DNA were digested by incubation of the lysate with salt-active nuclease (ArcticZymes) for 1 h followed by PEG-precipitation of proteins, including AAVs, for 3 h. The PEG pellet was resuspended overnight and AAVs were purified by an iodixanol gradient to remove contaminating proteins and empty capsids. After exchanging the buffer and simultaneously concentrating the AAV-containing iodixanol fraction using Amicon Ultra-15 filtration tubes (Merck), the concentrate was sterile filtered.

AAV titer determination by dPCR

Viral genomes were isolated with ViralXpress DNA/RNA Extraction Reagent (Merck) and serially diluted in nuclease-free H₂O. We transferred 7.0 μ L of dilutions 5.0×10^{-3} – 7.81×10^{-7} to a 96-well plate. Master Mix was prepared with 3.0 μ L of 4 \times Probe Master Mix (Qiagen), 0.6 μ L FAM-labeled 20 \times Primer Probe mix targeting AAV2-ITR (forward primer: GGAACCCCTAGTGATGGAGTT, reverse primer: CGGCCTCAGTGAGCGA, probe: CACTCCCTCTCTGC GCGCTCG) and 1.4 μ L nuclease-free H₂O. We added 5 μ L Master mix to each sample dilution and mixed before transferring 12 μ L sample mix into 96-well Nanoplate 8.5k (Qiagen). After sealing the plate, viral genomes were amplified by using a QIAcuity One instrument (Qiagen) and running a PCR with the following cycling conditions: 95°C for 10 min followed by 40 cycles of 95°C for 15 s and 60°C for 1 min. After completion of PCR, partitions were imaged with an 800-ms exposure time, with the gain set to 6. Data analysis was performed using QIAcuity software Suite version 2.5.0.1.

Statistics

Statistical analyses were performed using GraphPad Prism 9.5 (GraphPad). Statistical significance was determined using the tests specified in the respective figure legends and expressed as follows: * $p < 0.05$, ** $p < 0.01$, *** $p < 0.001$ and **** $p < 0.0001$. Results are shown as mean \pm SD.

DATA AND CODE AVAILABILITY

The data that support the findings of this study are available within this study or available from the corresponding author B.S. upon reasonable request.

ACKNOWLEDGMENTS

This work was supported by Boehringer Ingelheim Pharma GmbH & Co. KG, Biberach, Germany.

AUTHOR CONTRIBUTIONS

G.B.: investigation, formal analysis, methodology, visualization, writing – original draft, writing – review and editing; C.M.: investigation; M.L. writing – review and editing; J.Z.: resources, writing – review and editing; B.S.: conceptualization, methodology, supervision, project administration, writing – original draft, writing – review and editing.

DECLARATION OF INTERESTS

G.B., C.M., M.L., and B.S. are employees of Boehringer Ingelheim Pharma GmbH & Co. KG, Biberach, Germany.

REFERENCES

- Mingozzi, F., and High, K.A. (2013). Immune responses to AAV vectors: overcoming barriers to successful gene therapy. *Blood* 122, 23–36. <https://doi.org/10.1182/blood-2013-01-306647>.
- Xiao, X., Li, J., and Samulski, R.J. (1996). Efficient long-term gene transfer into muscle tissue of immunocompetent mice by adeno-associated virus vector. *J. Virol.* 70, 8098–8108. <https://doi.org/10.1128/jvi.70.11.8098-8108.1996>.
- Sehara, Y., Fujimoto, K.I., Ikeguchi, K., Katakai, Y., Ono, F., Takino, N., Ito, M., Ozawa, K., and Muramatsu, S.I. (2017). Persistent Expression of Dopamine-Synthesizing Enzymes 15 Years After Gene Transfer in a Primate Model of Parkinson's Disease. *Hum. Gene Ther. Clin. Dev.* 28, 74–79. <https://doi.org/10.1089/humc.2017.010>.
- Strobel, B., Duechs, M.J., Schmid, R., Stierstorfer, B.E., Bucher, H., Quast, K., Stiller, D., Hildebrandt, T., Mennerich, D., Gantner, F., et al. (2015). Modeling Pulmonary Disease Pathways Using Recombinant Adeno-Associated Virus 6.2. *Am. J. Respir. Cell Mol. Biol.* 53, 291–302. <https://doi.org/10.1165/rcmb.2014-0338ma>.
- Roche-Molina, M., Sanz-Rosa, D., Cruz, F.M., García-Prieto, J., López, S., Abia, R., Muriana, F.J.G., Fuster, V., Ibáñez, B., and Bernal, J.A. (2015). Induction of Sustained Hypercholesterolemia by Single Adeno-Associated Virus-Mediated Gene Transfer of Mutant hPCSK9. *Arterioscler. Thromb. Vasc. Biol.* 35, 50–59. <https://doi.org/10.1161/atvbaha.114.303617>.
- Cideciyan, A.V., Hauswirth, W.W., Aleman, T.S., Kaushal, S., Schwartz, S.B., Boye, S.L., Windsor, E.A.M., Conlon, T.J., Sumaroka, A., Pang, J.J., et al. (2009). Human RPE65 Gene Therapy for Leber Congenital Amaurosis: Persistence of Early Visual Improvements and Safety at 1 Year. *Hum. Gene Ther.* 20, 999–1004. <https://doi.org/10.1089/hum.2009.086>.
- Werfel, S., Jungmann, A., Lehmann, L., Ksienzyk, J., Bekeredjian, R., Kaya, Z., Leuchs, B., Nordheim, A., Backs, J., Engelhardt, S., et al. (2014). Rapid and highly efficient inducible cardiac gene knockout in adult mice using AAV-mediated expression of Cre recombinase. *Cardiovasc. Res.* 104, 15–23. <https://doi.org/10.1093/cvr/cvu174>.
- Chen, X., Ravindra Kumar, S., Adams, C.D., Yang, D., Wang, T., Wolfe, D.A., Arokiaaraj, C.M., Ngo, V., Campos, L.J., Griffiths, J.A., et al. (2022). Engineered AAVs for non-invasive gene delivery to rodent and non-human primate nervous systems. *Neuron* 110, 2242–2257.e6. <https://doi.org/10.1016/j.neuron.2022.05.003>.
- Urabe, M., Ding, C., and Kotin, R.M. (2002). Insect Cells as a Factory to Produce Adeno-Associated Virus Type 2 Vectors. *Hum. Gene Ther.* 13, 1935–1943. <https://doi.org/10.1089/10430340260355347>.
- Merten, O.-W. (2024). Development of Stable Packaging and Producer Cell Lines for the Production of AAV Vectors. *Microorganisms* 12, 384. <https://doi.org/10.3390/microorganisms12020384>.
- Kotterman, M.A., and Schaffer, D.V. (2014). Engineering adeno-associated viruses for clinical gene therapy. *Nat. Rev. Genet.* 15, 445–451. <https://doi.org/10.1038/nrg3742>.
- Au, H.K.E., Isalan, M., and Mielcarek, M. (2021). Gene Therapy Advances: A Meta-Analysis of AAV Usage in Clinical Settings. *Front. Med.* 8, 809118. <https://doi.org/10.3389/fmed.2021.809118>.
- Strobel, B., Klausner, B., Hartig, J.S., Lamla, T., Gantner, F., and Kreuz, S. (2015). Riboswitch-mediated Attenuation of Transgene Cytotoxicity Increases Adeno-associated Virus Vector Yield in HEK-293 Cells. *Mol. Ther.* 23, 1582–1591. <https://doi.org/10.1038/mt.2015.123>.
- Reid, C.A., Boye, S.L., Hauswirth, W.W., and Lipinski, D.M. (2017). miRNA-mediated post-transcriptional silencing of transgenes leads to increased adeno-associated viral vector yield and targeting specificity. *Gene Ther.* 24, 462–469. <https://doi.org/10.1038/gt.2017.50>.
- Wightman, B., Ha, I., and Ruvkun, G. (1993). Posttranscriptional regulation of the heterochronic gene *lin-14* by *lin-4* mediates temporal pattern formation in *C. elegans*. *Cell* 75, 855–862. [https://doi.org/10.1016/0092-8674\(93\)90530-4](https://doi.org/10.1016/0092-8674(93)90530-4).
- Lee, R.C., Feinbaum, R.L., and Ambros, V. (1993). The *C. elegans* heterochronic gene *lin-4* encodes small RNAs with antisense complementarity to *lin-14*. *Cell* 75, 843–854. [https://doi.org/10.1016/0092-8674\(93\)90529-y](https://doi.org/10.1016/0092-8674(93)90529-y).
- Liu, J., Carmell, M.A., Rivas, F.V., Marsden, C.G., Thomson, J.M., Song, J.-J., Hammond, S.M., Joshua-Tor, L., and Hannon, G.J. (2004). Argonaute2 Is the Catalytic Engine of Mammalian RNAi. *Science* 305, 1437–1441. <https://doi.org/10.1126/science.1102513>.
- Hutvagner, G., and Zamore, P.D. (2002). A microRNA in a Multiple-Turnover RNAi Enzyme Complex. *Science* 297, 2056–2060. <https://doi.org/10.1126/science.1073827>.
- McBride, J.L., Boudreau, R.L., Harper, S.Q., Staber, P.D., Monteys, A.M., Martins, L., Gilmore, B.L., Burstein, H., Peluso, R.W., Polisky, B., et al. (2008). Artificial miRNAs mitigate shRNA-mediated toxicity in the brain: Implications for the therapeutic development of RNAi. *Proc. Natl. Acad. Sci. USA* 105, 5868–5873. <https://doi.org/10.1073/pnas.0801775105>.
- Guda, S., Brendel, C., Renella, R., Du, P., Bauer, D.E., Canver, M.C., Grenier, J.K., Grimson, A.W., Kamran, S.C., Thornton, J., et al. (2015). miRNA-embedded shRNAs for Lineage-specific BCL11A Knockdown and Hemoglobin F Induction. *Mol. Ther.* 23, 1465–1474. <https://doi.org/10.1038/mt.2015.113>.
- Grimm, D., Streetz, K.L., Jopling, C.L., Storm, T.A., Pandey, K., Davis, C.R., Marion, P., Salazar, F., and Kay, M.A. (2006). Fatality in mice due to oversaturation of cellular microRNA/short hairpin RNA pathways. *Nature* 441, 537–541. <https://doi.org/10.1038/nature04791>.
- Khan, A.A., Betel, D., Miller, M.L., Sander, C., Leslie, C.S., and Marks, D.S. (2009). Transfection of small RNAs globally perturbs gene regulation by endogenous microRNAs. *Nat. Biotechnol.* 27, 549–555. <https://doi.org/10.1038/nbt.1543>.
- Fellmann, C., Hoffmann, T., Sridhar, V., Hopfgartner, B., Muhar, M., Roth, M., Lai, D.Y., Barbosa, I.A.M., Kwon, J.S., Guan, Y., et al. (2013). An Optimized microRNA Backbone for Effective Single-Copy RNAi. *Cell Rep.* 5, 1704–1713. <https://doi.org/10.1016/j.celrep.2013.11.020>.
- Pelossof, R., Fairchild, L., Huang, C.-H., Widmer, C., Sreedharan, V.T., Sinha, N., Lai, D.-Y., Guan, Y., Premisrirut, P.K., Tschaharganeh, D.F., et al. (2017). Prediction of potent shRNAs with a sequential classification algorithm. *Nat. Biotechnol.* 35, 350–353. <https://doi.org/10.1038/nbt.3807>.
- Fang, W., and Bartel, D.P. (2015). The Menu of Features that Define Primary MicroRNAs and Enable De Novo Design of MicroRNA Genes. *Mol. Cell* 60, 131–145. <https://doi.org/10.1016/j.molcel.2015.08.015>.
- Petri, S., and Meister, G. (2013). siRNA design principles and off-target effects. *Methods Mol. Biol.* 986, 59–71. https://doi.org/10.1007/978-1-62703-311-4_4.
- Renault, T.T., and Manon, S. (2011). Bax: Addressed to kill. *Biochimie* 93, 1379–1391. <https://doi.org/10.1016/j.biochi.2011.05.013>.
- Griesser, E., Schönberger, T., Stierstorfer, B., Wyatt, H., Rist, W., Lamla, T., Thomas, M.J., Lamb, D., and Geillinger-Kästle, K. (2022). Characterization of a flexible AAV-DTR/DT mouse model of acute epithelial lung injury. *Am. J. Physiol. Lung Cell Mol. Physiol.* 323, L206–L218. <https://doi.org/10.1152/ajplung.00364.2021>.
- Qiu, X., Friedman, J.M., and Liang, G. (2011). Creating a flexible multiple microRNA expression vector by linking precursor microRNAs. *Biochem. Biophys. Res. Commun.* 411, 276–280. <https://doi.org/10.1016/j.bbrc.2011.06.123>.
- Furukawa, N., Sakurai, F., Katayama, K., Seki, N., Kawabata, K., and Mizuguchi, H. (2011). Optimization of a microRNA expression vector for function analysis of microRNA. *J. Control. Release* 150, 94–101. <https://doi.org/10.1016/j.jconrel.2010.12.001>.
- Liu, H., Aramaki, M., Fu, Y., and Forrest, D. (2017). Retinoid-Related Orphan Receptor β and Transcriptional Control of Neuronal Differentiation. *Curr. Top. Dev. Biol.* 125, 227–255. <https://doi.org/10.1016/bs.ctdb.2016.11.009>.
- Jin, H., Zhang, C., Zwahlen, M., von Feilitzen, K., Karlsson, M., Shi, M., Yuan, M., Song, X., Li, X., Yang, H., et al. (2023). Systematic transcriptional analysis of human cell lines for gene expression landscape and tumor representation. *Nat. Commun.* 14, 5417. <https://doi.org/10.1038/s41467-023-41132-w>.
- Strobel, B., Düchs, M.J., Blazevic, D., Rechtsteiner, P., Braun, C., Baum-Kroker, K.S., Schmid, B., Ciossek, T., Gottschling, D., Hartig, J.S., and Kreuz, S. (2020). A Small-Molecule-Responsive Riboswitch Enables Conditional Induction of Viral Vector-Mediated Gene Expression in Mice. *ACS Synth. Biol.* 9, 1292–1305. <https://doi.org/10.1021/acssynbio.9b00410>.

34. Prasad, K.-M.R., Xu, Y., Yang, Z., Acton, S.T., and French, B.A. (2011). Robust cardiomyocyte-specific gene expression following systemic injection of AAV: *in vivo* gene delivery follows a Poisson distribution. *Gene Ther.* *18*, 43–52. <https://doi.org/10.1038/gt.2010.105>.
35. Kügler, S., Lingor, P., Schöll, U., Zolotukhin, S., and Bähr, M. (2003). Differential transgene expression in brain cells *in vivo* and *in vitro* from AAV-2 vectors with small transcriptional control units. *Virology* *311*, 89–95. [https://doi.org/10.1016/s0042-6822\(03\)00162-4](https://doi.org/10.1016/s0042-6822(03)00162-4).
36. Graham, T., McIntosh, J., Work, L.M., Nathwani, A., and Baker, A.H. (2008). Performance of AAV8 vectors expressing human factor IX from a hepatic-selective promoter following intravenous injection into rats. *Genet. Vaccines Ther.* *6*, 9. <https://doi.org/10.1186/1479-0556-6-9>.
37. Wiggins, J.F., Ruffino, L., Kelnar, K., Omotola, M., Patrawala, L., Brown, D., and Bader, A.G. (2010). Development of a Lung Cancer Therapeutic Based on the Tumor Suppressor MicroRNA-34. *Cancer Res.* *70*, 5923–5930. <https://doi.org/10.1158/0008-5472.can-10-0655>.
38. Hordeaux, J., Buza, E.L., Jeffrey, B., Song, C., Jahan, T., Yuan, Y., Zhu, Y., Bell, P., Li, M., Chichester, J.A., et al. (2020). MicroRNA-mediated inhibition of transgene expression reduces dorsal root ganglion toxicity by AAV vectors in primates. *Sci. Transl. Med.* *12*, eaba9188. <https://doi.org/10.1126/scitranslmed.aba9188>.
39. Subramanian, M., McIninch, J., Zlatev, I., Schlegel, M.K., Kaittanis, C., Nguyen, T., Agarwal, S., Racie, T., Alvarado, M.A., Wassarman, K., et al. (2023). RNAi-mediated rheostat for dynamic control of AAV-delivered transgenes. *Nat. Commun.* *14*, 1970. <https://doi.org/10.1038/s41467-023-37774-5>.
40. Limb, G.A., Salt, T.E., Munro, P.M.G., Moss, S.E., and Khaw, P.T. (2002). *In vitro* characterization of a spontaneously immortalized human Müller cell line (MIO-M1). *Invest. Ophthalmol. Vis. Sci.* *43*, 864–869.
41. Strobel, B., Zuckschwerdt, K., Zimmermann, G., Mayer, C., Eytner, R., Rechtsteiner, P., Kreuz, S., and Lamla, T. (2019). Standardized, Scalable, and Timely Flexible Adeno-Associated Virus Vector Production Using Frozen High-Density HEK-293 Cell Stocks and CELLdiscs. *Hum. Gene Ther. Methods* *30*, 23–33. <https://doi.org/10.1089/hgtb.2018.228>.